Evaluation of the field-scale cation exchange capacity of Hanford sediments

C.I. Steefel
Earth Sciences Division, Lawrence Berkeley National Laboratory, Berkeley, CA USA

ABSTRACT: Three-dimensional simulations of unsaturated flow, transport, and multi-component, multi-site cation exchange in the vadose zone were used to analyze the migration of a plume resulting from a leak of the SX-115 tank at the Hanford site, USA. The match within about 0.5 meters of the positions of retarded sodium and potassium fronts suggests that the laboratory-derived parameters may be used in field-scale simulations of radionuclide migration at the Hanford site.

1 INTRODUCTION

The chromatographic separation of contaminants as a result of multi-component cation exchange is a well-known effect in both soils and subsurface sediments (Valocchi et al. 1981a, b, Appelo & Willemsen 1987, Charbeneau 1988, Griffioen et al. 1992, Appelo & Postma 1993, Appelo 1996, Voegelin et al. 2000, Steefel et al. 2003). Although ion exchange parameters extracted from batch (Zachara et al. 2002) and column experiments (Steefel et al. 2003) provide an excellent basis for modeling the reactive transport of radionuclides such as cesium under experimental conditions, the same cation exchange model may not be capable of describing transport at the field-scale. Of key concern is whether the effective cation exchange capacity in the field is the same as that determined for bulk composites samples used in laboratory column experiments (Steefel et al. 2003). A number of processes or effects could cause the effective cation exchange capacity in the field to be different from (and generally less than) the values measured in one-dimensional fully saturated laboratory experiments: (1) the subsurface exchange capacity may not be distributed homogeneously, (2) multi-scale physical heterogeneities could lead to by-passing of the exchange capacity by the water flow, and (3) relatively immobile regions characterized by very little flow and transport could develop, particularly at low water saturations.

To evaluate the effective cation exchange capacity of Hanford sediments at the field scale, a plume developed in the vadose zone below a leak in the SX-115 high-level waste tank was modeled. The advantage of considering the SX-115 leak is that both its volume (~ 216,030 liters) and duration (1 week in 1965) are well known. Through analysis of water extractable ions, Serne et al. (2001) identified a well-defined chromatographic separation of cations in 299-W23-19, a borehole sited approximately two meters from the edge of the SX-115 tank, which can be attributed to the exchange of waste-derived cations. A peak of sodium occurs in the borehole that is clearly separated from calcium and magnesium peaks at greater depth. Potassium also shows some retardation. Technetium and nitrate, apparently acting as non-reactive tracers, coincided approximately with the calcium and magnesium fronts. The small but measurable retardations of sodium and potassium, although not of significant interest as contaminants themselves, provide an opportunity to quantify the effective field-scale cation exchange capacity of the Hanford sediments.

2 MULTI-COMPONENT, MULTI-SITE CATION EXCHANGE FORMULATION

Multi-component cation exchange was formulated using the Gaines-Thomas activity convention, which assumes a reaction stoichiometry of the following form (Appelo & Postma 1993):

$$Cs^{+} + \tfrac{1}{m} MX(i)_m \leftrightarrow CsX(i) + \tfrac{1}{m} M^{m+}, \qquad (1)$$

where M is the competing cation (Na^{+}, K^{+}, Ca^{++}), m is its charge, and $X(i)$ refers to the i^{th} type of exchange site. The activities of adsorbed species correspond to the charge equivalent fractions:

$$\beta(i)_M = \frac{z_M q(i)_M}{\sum_M z_M q(i)_M} = [X(i)_M], \qquad (2)$$

where z_M is the charge of cation M, $q(i)_M$ is the concentration of adsorbed cation M in exchange site i (moles/g), and the square brackets denote activities. The exchange reactions can then be used to write a mass action equation for binary Cs-M exchange:

$$K_{M/Cs} = \frac{\beta(i)_M^{1/m}[Cs^+]}{\beta(i)_{Cs}[M^{m+}]^{1/m}} = \frac{[X(i)_M]^{1/m}[Cs^+]}{[X(i)_{Cs}][M^{m+}]^{1/m}}. \quad (3)$$

As noted by Zachara et al. (2002), multiple exchange sites are needed to capture the large range in the distribution coefficient for Cs^+ as a function of Cs^+ concentration. Zachara et al. (2002) used a model to fit the data including two sites: one a site with a high selectivity for Cs^+ associated with the frayed edges sites (FES) on weathered micas and a second with a relatively lower selectivity Cs^+ associated with the surfaces of expansible layer silicates. Steefel et al. (2003) compared the fits obtained with two-site and three-site models and concluded that the three-site model offered a slightly better fit of both the batch exchange data and self-sharpened breakthrough curves in column experiments at low Cs^+ concentrations. In this analysis, Steefel et al. (2003) assumed that the total cation exchange capacity determined independently by ^{22}Na exchange in a flow-through column experiment as 120 μeq/g corresponded to the abundant sites developed on expansible clays, whereas the less abundant one or two FES sites (constituting less than 1% of the total cation exchange capacity) were fitted along with the selectivity coefficients. Results are summarized in Table 1.

Table 1: Selectivity coefficients and site concentrations based on fit of column and batch data (Steefel et al. 2003).

Exchange Reaction		Log Selectivity Coefficient
$NaX1 + Cs^+ = Na^+ + CsX1$		7.25
$NaX2 + Cs^+ = Na^+ + CsX2$		4.93
$NaX3 + Cs^+ = Na^+ + CsX3$		1.99
$KX1 + Cs^+ = K^+ + CsX1$		4.99
$KX2 + Cs^+ = K^+ + CsX2$		1.83
$KX3 + Cs^+ = K^+ + CsX3$		0.74
$0.5CaX1_2 + Cs^+ = 0.5Ca^{2+} + CsX1$		15.27
$0.5CaX2_2 + Cs^+ = 0.5Ca^{2+} + CsX2$		10.89
$0.5CaX3_2 + Cs^+ = 0.5Ca^{2+} + CsX3$		3.20
Exchange Site	(μeq g^{-1})	% of CEC
Site 1 (FES)	0.02	0.02
Site 2 (FES)	0.26	0.22
Site 3 (planar)	120	99.76
CEC	120.28	

3 SIMULATIONS OF THE SX-115 TANK LEAK

The SX-115 tank leak and subsequent plume migration through the vadose zone was modeled by coupling the reactive transport code CRUNCH (Steefel 2001) to the multiphase flow and heat transport code NUFT (Nitao 1998). CRUNCH reads in a transient flow, liquid saturation, and temperature fields generated by NUFT. The simulation begins in 1959 when the SX-115 tank was constructed and ends in the year 1999 when borehole 299-W23-19 was drilled. A 3-D grid was considered necessary to capture the potential effects of a dipping gravel layer and the lack of symmetry with respect to the large leak located on the edge of the tank near borehole 299-W23-19. Nineteen and 17 cells of 2.33 meter spacing were used in the X and Y direction respectively, whereas 34 cells of 2 meter spacing were used in the Z (vertical) direction. The SX-115 tank was maintained at a constant temperature of 70°C throughout the period of the simulation (1959-1999). The data of Raymond & Shdo (1966) indicate that three distinct leaks developed below the SX-115 tank. Although it is not clear that all three of them leaked during the same one week period in 1965, an assumption has been made that the largest of the leaks developed on the edge of the tank near Well 299-W23-19 (the only one modeled here) and consisted of 86,412 liters, 40% of the total 216,030 liters lost during this period.

3.1 *Flow & heat transport simulations*

Hydrologic parameters used in the simulations are those given in Khaleel et al. (2001). These flow and transport parameters represent effective (upscaled) values for the Hanford vadose zone and are broken out by the strata present at the S-SX tank farms (Table 2).

The distribution of model permeabilities is shown in an X-Z section through the SX-115 tank and 299-W23-19 borehole (Fig. 1). Except for the backfill, all the strata were assumed to have horizontal conductivities three times their vertical conductivities. Based on the shape of cesium contamination detected in horizontal boreholes 3.05 meters below SX-115 (Raymond & Shdo 1966), the assumption of an anistropy ratio of 3:1 appears to be reasonable. A larger anisotropy ratio would have spread the cesium contamination horizontally farther than is observed, if it is assumed that the retardation of cesium is approximately the same in the horizontal and vertical directions. The tank was assumed to be impermeable. Boundary conditions for the simulation consisted of no–flow boundaries on the side of the domain and fixed pressure boundary conditions at the bottom (the water table, which is assumed to have a fixed depth) and the surface. A constant infiltration rate of 100 mm/year is assumed at the top of the domain.

3.2 *Chemical initial & boundary conditions*

The major point of the modeling exercise described here is to see how well various geochemical parameters taken from column experiments (Steefel et al. 2003) can be used to describe the field transport of cesium and the other relevant cations. In addition, their

behavior can be used as a partial test of the multi-component ion exchange model. Accordingly, an effort was made to minimize calibration of the model to evaluate directly the applicability of the experimental studies to the field.

The boundary condition at the top of the domain was assumed to be the same as the initial aqueous concentration. More important is the composition of the fluid leaking from the tank. Lichtner & Felmy (2003) have estimated tank compositions based on reaction path modeling of the tank liquors. Their results for the SX-115 tank were used as a "base case" for the simulations. A variety of runs were carried out by diluting the "base case" tank composition.

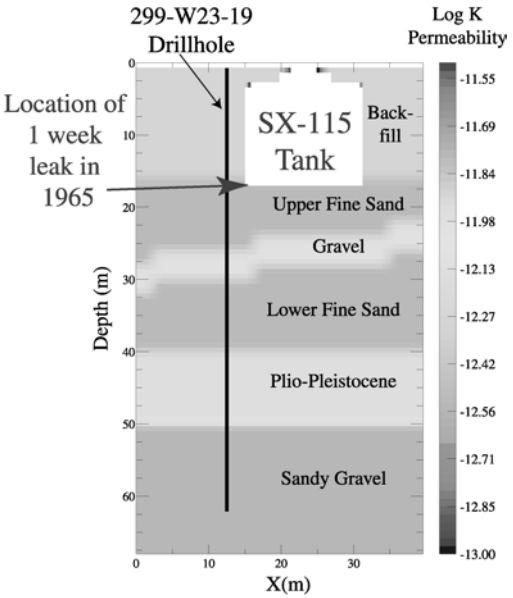

Figure 1. Permeability distribution used in 3D simulations

4 RESULTS

Results represent a preliminary attempt to verify that the cation exchange parameters determined from batch and column experiments can be combined with hydrologic parameters appropriate for the Hanford Formation to describe Na, K, Ca, Mg, and to a lesser extent Cs reactive transport in Hanford sediments. Technetium and nitrate serve as non-reactive tracers that can be used to assess how accurately the flow regime is captured.

A direct comparison of aqueous geochemical data collected from the 299-W23-19 borehole and the simulations is shown in Figure 2. The simulations capture quite closely the leading edge of all the exchange fronts, although the match with the trailing portions of the plumes was not as accurate. However, the simulations capture some aspects of the complicated shape of the cation plumes, including the sodium "shoulder" above the main part of the sodium plume in the aqueous phase. This presumably represents sodium being gradually eluted from exchange sites above the main zone of sodium in the aqueous phase. The simulated widths of the magnesium and calcium plumes were slightly too broad, although this may be the result of an overly coarse discretization. The relatively broader shape of the potassium plume, which shows up clearly in the data, is captured in an approximate fashion by the simulations. Cesium, although not detected in significant amounts in the 299-W23-19 borehole, is known to occur very close to the bottom of the SX-115 tank (Raymond & Shdo 1966).

These results do not include any calibration of either the independently estimated hydrologic parameters (taken directly from Khaleel et al. 2001) or the laboratory-determined cation exchange capacity and ion exchange selectivity coefficients. In order to match the absolute concentration of sodium in the borehole, the composition of the tank leak fluid was adjusted, however, with a "best fit" value representing a dilution of the estimate provided by Lichtner & Felmy (2003) by about a factor of 3.5. The exchange calcium concentration required almost no adjustment from the value determined experimentally, but the exchange concentration of magnesium determined in the column experiments was adjusted downward by about a factor of 2 to obtain a match with the field data. Potassium was increased by a factor of 2 to 4 over the values estimated from the column experiments.

5 CONCLUSIONS

Flow and reactive transport modeling of the SX-115 leak, which developed in 1965 indicates that the cation exchange model developed by Zachara et al. (2002) and Steefel et al. (2003) provides an excellent basis for field simulations of cation exchange. The well-defined chromatographic separation of the cations in the field clearly demonstrates that the effective field cation exchange capacity is close to the value determined independently in the batch and column experiments. Various hydrologic mechanisms for "bypassing" exchange sites (fast flow pathways or transport-limited sorption in immobile water zones), while not necessarily discounted altogether, do not appear to have had a large effect on the extent of cation exchange.

REFERENCES

Appelo, C.A.J. 1996. Multicomponent ion exchange and chromatography in natural systems. In P.C. Lichtner, C.I. Steefel & E.H. Oelkers (eds.), *Reactive Transport in Porous Media. Reviews in Mineralogy* 34: 193-227.

Appelo, C.A.J. & Postma, D. 1993. *Geochemistry, Groundwater, and Pollution*. Rotterdam: A.A. Balkema.

Appelo, C.A.J. & Willemsen, A. 1987. Geochemical calculations and observations on salt water intrusions, I. *Journal of Hydrology* 94: 313-330.

Charbeneau, R.J. 1988. Multicomponent exchange and subsurface solute transport: characteristics, coherence and the Reimann problem. *Water Resources Research* 24: 57-64.

Doherty, J., Lindsay, B. & Whyte, P. 1994. PEST: *Model Independent Parameter Estimation*. Brisbane, Australia: Watermark Computing.

Griffioen, J., Appelo, C.A.J. & van Veldhuizen, M. 1992. Practice of chromatography: deriving isotherms from elution curves. *Soil Science Society of America Journal* 56: 1429-1437.

Khaleel, R., Jones, T. E., Knepp, A. J., Mann, F. M., Myers, D. A., Rogers, P. M., Serne, R. J. & Wood, M. I. 2000. Modeling Data Package for S-SX Field Investigation Report (FIR), *RPP-6296, Rev. 0*. Richland, WA: CH2M Hill Hanford Group, Inc.

Lichtner, P.C. & Felmy, A.R. 2003. Estimation of Hanford SX tank waste compositions from historically derived inventories. *Computers & Geosciences* 29: 371-383.

Nitao, J. 1998, Reference Manual for the NUFT Flow and Transport Code, Version 2.0, *UCRL-MA-130651*, Livermore, CA: Lawrence Livermore National Laboratory.

Serne, R.J., Schaef, H.T., Bjornstad, B.N., Lanigan, D.C., Gee, G.W., Lindenmeier, C.W., Clayton, R.E., LeGore, V.L., O'Hara, M.J., Brown, C.F., Orr, R.D., Last, G.V., Kutnyakov, I.V., Burke, D.B., Wilson, T.C. & Williams, B.A. 2001. Geologic and geochemical data collected from vadose zone sediments from borehole 299 W23-19 [SX -115] In *the S/SX Waste Management Area and Preliminary Interpretations.* PNNL-2001-3. Richland, Washington: Pacific Northwest National Laboratory.

Raymond, J. R. & Shdo, E. D. 1966, Characterization of Subsurface Contamination in the SX Tank Farm. *BNWl-CC-701*, Richland, WA.

Steefel, C.I. 2001. GIMRT, version 1.2: Software for modeling multicomponent, multidimensional reactive transport. User's Guide, *UCRL-MA-143182*. Livermore, California: Lawrence Livermore National Laboratory.

Steefel, C.I., Carroll S.A., Zhao, P. & Roberts, S. 2003. Cesium migration in Hanford sediments: a multisite cation exchange model based on laboratory transport experiments. *Journal of Contaminant Hydrology* 67: 219-246.

Valocchi, A.J., Roberts, P.V., Parks, G.A. & Street, R.L. 1981a. Simulation of the transport of ion-exchanging solutes using laboratory-determined chemical parameter values. *Ground Water* 19: 600-607.

Valocchi, A.J., Street, R.L. & Roberts, P.V. 1981b. Transport of ion-exchanging solutes in groundwater: chromatographic theory and field simulation. *Water Resources Research* 17: 1517-1527.

Zachara, J.M., Smith, S.C., Liu, C., McKinley, J.P., Serne, R.J. & Gassman, P.L. 2002. Sorption of Cs^+ to micaceous subsurface sediments from the Hanford site, USA. *Geochimica Cosmochimca Acta* 66: 193-211.

Table 2. Composite van Genuchten-Mualem parameters for various strata at the S-SX tank farms (Khaleel et al. 2001).

Strata	Porosity	Residual Water Content	α (1/cm)	n	Vertical Ks (cm/s)	Horizontal Ks (cm/s)
Backfill	0.2688	0.0151	0.0197	1.4194	5.15E-04	5.15E-04
Fine sand (upper and lower)	0.3819	0.0443	0.0117	1.6162	9.88E-05	2.96E-04
Gravelly sand-sandy gravel	0.2126	0.0032	0.0141	1.3730	2.62E-04	7.86E-04
Plio-pleistocene	0.4349	0.0665	0.0085	1.8512	2.40E-04	7.20E-04
Sandy gravel	0.1380	0.0100	0.0210	1.3740	5.60E-04	1.68E-03

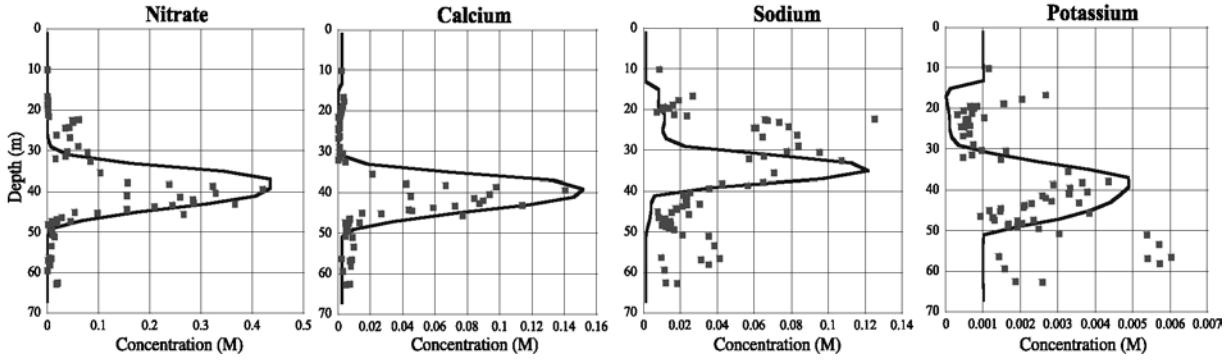

Figure 2. Comparison of 3D modeling results with pore water extracts from Borehole 299-W23-19 below the SX-115 tank.